

***Streptococcus pneumoniae* evades host cell phagocytosis and limits host mortality
through its cell wall anchoring protein PfbA**

Running title: PfbA inhibits phagocytosis and limits host responses

Masaya Yamaguchi^{a, #}, Yujiro Hirose^a, Moe Takemura^{a, b}, Masayuki Ono^{a, c}, Tomoko
Sumitomo^a, Masanobu Nakata^a, Yutaka Terao^d, Shigetada Kawabata^a

^aDepartment of Oral and Molecular Microbiology, Osaka University Graduate School of
Dentistry, Osaka, Japan

^bDepartment of Oral and Maxillofacial Surgery II, Osaka University Graduate School of
Dentistry, Osaka, Japan

^cDepartment of Fixed Prosthodontics, Osaka University Graduate School of Dentistry,
Osaka, Japan.

^dDivision of Microbiology and Infectious Diseases, Niigata University Graduate School
of Medical and Dental Sciences, Niigata, Japan

17 #Address correspondence to Masaya Yamaguchi, yamaguchi@dent.osaka-u.ac.jp

18

19 Word count: 5255 words

Abstract

Streptococcus pneumoniae is a Gram-positive bacterium belonging to the oral streptococcus species, mitis group. This pathogen is a leading cause of community-acquired pneumonia, which often evades host immunity and causes systemic diseases, such as sepsis and meningitis. Previously, we reported that PfbA is a β -helical cell surface protein contributing to pneumococcal adhesion to and invasion of human epithelial cells in addition to its survival in blood. In the present study, we investigated the role of PfbA in pneumococcal pathogenesis. Phylogenetic analysis indicated that the *pfbA* gene is specific to *S. pneumoniae* within the mitis group. Our *in vitro* assays showed that PfbA inhibits neutrophil phagocytosis, leading to pneumococcal survival. We found that PfbA activates NF- κ B through TLR2, but not TLR4. In addition, TLR2/4 inhibitor peptide treatment of neutrophils enhanced the survival of the *S. pneumoniae* $\Delta pfbA$ strain as compared to a control peptide treatment, whereas the treatment did not affect survival of a wild-type strain. In a mouse pneumonia model, the host mortality and level of TNF- α in bronchoalveolar lavage fluid were comparable between wild-type and $\Delta pfbA$ -infected mice, while deletion of

pfbA increased the bacterial burden in bronchoalveolar lavage fluid. In a mouse sepsis model, the $\Delta pfbA$ strain demonstrated significantly increased host mortality and TNF- α levels in plasma, but showed reduced bacterial burden in lung and liver. These results indicate that PfbA may contribute to the success of *S. pneumoniae* species by inhibiting host cell phagocytosis, excess inflammation, and mortality.

Importance

Streptococcus pneumoniae is often isolated from the nasopharynx of healthy children, but the bacterium is also a leading cause of pneumonia, meningitis, and sepsis. In this study, we focused on the role of a cell wall anchoring protein, PfbA, in the pathogenesis of *S. pneumoniae*-related disease. We found that PfbA is a pneumococcus-specific anti-phagocytic factor that functions as a TLR2 ligand, indicating that PfbA may represent a pneumococcal-specific therapeutic target. However, a mouse pneumonia model revealed that PfbA deficiency reduced the bacterial burden, but did not decrease host mortality. Furthermore, in a mouse sepsis model, PfbA deficiency increased host mortality. These results suggest that *S.*

pneumoniae optimizes reproduction by regulating host mortality through PfbA; therefore, PfbA inhibition would not be an effective strategy for combatting pneumococcal infection. Our findings underscore the challenges involved in drug development for a bacterium harboring both commensal and pathogenic states.

Introduction

Streptococcus pneumoniae is Gram-positive bacteria belonging to the mitis group that colonizes the human nasopharynx in approximately 20% of children without causing clinical symptoms (1-3). On the other hand, *S. pneumoniae* is also a leading cause of bacterial pneumonia, meningitis, and sepsis worldwide. The pathogen is estimated to be responsible for the deaths of approximately 1,190,000 people annually from lower respiratory infection (4). Following the introduction of pneumococcal conjugate vaccines, *S. pneumoniae* is still responsible for two thirds of all cases of meningitis (5). In addition, antibiotic selective pressure causes resistant pneumococcal clones to emerge and expand all over the world and the World Health Organization listed *S. pneumoniae* as one of antibiotic-resistant "priority pathogens" (6). Centers for

Disease Control and Prevention data from active bacterial core surveillance for 2009 to 2013 indicated that pneumococcal conjugate vaccines work as a useful tool against antibiotic resistance (7). However, these vaccines also generate selective pressure, and non-vaccine serotypes of *S. pneumoniae* are increasing worldwide (8, 9).

During the process of invasive infection, *S. pneumoniae* needs to evade host immunity and replicate in the host after colonization. In these steps, pneumococcal cell surface proteins work as adhesins and/or anti-phagocytic factors. There are two types of motifs for pneumococcal cell surface localization, a cell wall anchoring motif, LPXTG (10), and choline-binding repeats interacting with pneumococcal phosphorylcholine (11). Choline-binding proteins (CBPs) localize on the pneumococcal cell wall via the phosphorylcholine moiety of teichoic acids, while LPXTG-anchored proteins are covalently attached to the cell wall. Several LPXTG-anchored proteins and CBPs contribute to the adhesion to host epithelial cells through the interaction with host factors (10-13). Some pneumococcal cell surface proteins also contribute to bacterial survival by limiting complement deposition or inhibiting phagocytosis (11, 14-17). On the other hand, the host recognizes *S. pneumoniae* and regulates immune responses

using pattern recognition receptors, including the Toll-like receptors (TLRs), nucleotide oligomerization domain-like receptors, and retinoic acid-inducible gene-I-like receptors (18). In addition, extracellular bacteria are recognized by TLR2 and TLR4 located on the host cell surface. TLR2 recognizes pneumococcal cell wall components and lipoproteins, while TLR4 senses a pore-forming toxin, pneumolysin (18, 19). Generally, both TLR2 and TLR4 agonists induce neutrophil activation and inhibit the apoptosis (20). However, in mouse influenza A virus and *S. pneumoniae* co-infection model, a TLR2 agonist decreased inflammation and reduced bacterial shedding and transmission (21). TLRs play important, but redundant, roles in the host defense and regulating inflammatory responses against pneumococcal infection. Appropriate immune responses contribute to pneumococcal clearance, while excessive inflammation can lead to serious tissue damage.

We previously reported that plasmin- and fibronectin-binding protein A (PfbA) plays a role in fibronectin-dependent adhesion to and invasion of epithelial cells, and that an *S. pneumoniae* PfbA-deficient mutant strain exhibited decreased survival in human blood (22, 23). PfbA is an LPXTG-anchored protein that features a right-handed

100 parallel β -helix with a groove or cleft, formed by three parallel β -sheets and connecting
 101 loops (24, 25). Since the distribution and structural arrangement of the groove residues
 102 in the β -helix make it favorable for binding to carbohydrates, PfbA binds to D-galactose,
 103 D-mannose, D-glucosamine, D-galactosamine, *N*-acetylneuraminic acid, D-sucrose, and
 104 D-raffinose (26). PfbA also binds to human erythrocytes by interacting with
 105 *N*-acetylneuraminic acids on the cells (27).

106 In this study, we investigated the role of PfbA in pneumococcal pathogenesis.
 107 Phylogenetic analysis indicated that *pfbA* is specific to *S. pneumoniae* among the mitis
 108 group *Streptococcus*. Our *in vitro* analysis revealed that PfbA works as an
 109 anti-phagocytic factor and that the protein causes NF- κ B activation via TLR2. In
 110 addition, Toll-interleukin 1 receptor adaptor protein (TIRAP) inhibition increased the
 111 survival rate of the *pfbA* mutant strain after incubation with neutrophils, while the
 112 wild-type (WT) strain was not affected. Mouse infection assays suggested that PfbA
 113 contributes to pneumococcal survival in at least some organs. However, in a mouse
 114 sepsis model, *pfbA* mutant strain-infected mice showed significantly higher mortality

115 and TNF- α levels in blood. Our findings indicate that PfbA is a pneumococcus-specific

116 anti-phagocytic factor and suppresses host excess inflammation.

117

118 **Materials and Methods**

119 **Bacterial strains and construction of mutant strain**

120 *Streptococcus pneumoniae* strains were cultured in Todd-Hewitt broth (BD
121 Biosciences, San Jose, CA, USA) supplemented with 0.2% yeast extract THY medium,
122 BD Biosciences) at 37°C. For selection and maintenance of mutants, spectinomycin
123 (Fujifilm Wako Pure Chemical Corporation, Osaka, Japan) was added to the medium at
124 120 µg/mL. The *Escherichia coli* strain XL10-Gold (Agilent, Santa Clara, CA, USA)
125 was used as a host for derivatives of plasmid pQE-30. All *E. coli* strains were cultured
126 in Luria-Bertani (LB) broth supplemented with 100 µg/mL carbenicillin (Nacalai
127 Tesque, Kyoto, Japan) at 37°C with agitation.

128 *S. pneumoniae* TIGR4 isogenic *pfbA* mutant strains were generated as previously
129 described with minor modifications (22, 28, 29). Briefly, the upstream region of *pfbA*,
130 an *aad9* cassette, the downstream region of *pfbA*, and pGEM-T Easy vector (Promega,
131 Madison, WI, USA) were amplified by PrimeSTAR[®] MAX DNA Polymerase (TaKaRa
132 Bio, Shiga, Japan) using the specific primers listed in Supplementary Table 1. The DNA
133 fragments were assembled using a GeneArt[®] Seamless Cloning and Assembly Kit
134 (Thermo Fisher Scientific, Waltham, MA, USA). The constructed plasmid was then

transformed into *E. coli* XL-10 Gold, and the inserted DNA region was amplified by PCR. The products were used to construct mutant strains by double-crossover recombination with the synthesized competence-stimulating peptide-2. The mutation was confirmed by PCR amplification of genomic DNA isolated from the mutant strain.

Cell culture

Human promyelocytic leukemia cells (HL-60, RCB0041) were purchased from RIKEN Cell Bank (Ibaraki, Japan). HL-60 cells were maintained in RPMI 1640 medium (Thermo Fisher Scientific) supplemented with 10% FBS, and were incubated at 37°C in 5% CO₂. HL-60 cells were differentiated into neutrophil-like cells for 5 days in culture media containing 1.2% DMSO (30, 31). Cell differentiation was confirmed by nitro blue tetrazolium reduction assay (30).

Human TLR2/NF-κB/SEAP stably transfected HEK293 cells and human TLR4/MD-2/CD14/NF-κB/SEAP stably transfected HEK293 cells (Novus Biologicals, Centennial, CO, USA, currently sold by InvivoGen, San Diego, CA, USA) were maintained in DMEM with 4.5 g/L glucose, 10% FBS, 4 mM L-glutamine, 1 mM

151 sodium pyruvate, 100 units/mL penicillin, 100 µg/mL streptomycin, 10 µg/mL
152 blasticidin, and 500 µg/mL G418 and DMEM with 4.5 g/L glucose, 10% FBS, 4 mM
153 L-glutamine, 1 mM sodium pyruvate, 100 units/mL penicillin, 100 µg/mL streptomycin,
154 10 µg/mL blasticidin, 2 µg/mL puromycin, 200 µg/mL zeocin, and 500 µg/mL G418,
155 respectively. A secreted alkaline phosphatase reporter assay was performed according to
156 the manufacturer's instructions (Novus Biologicals).

157

158 **Phylogenetic analysis**

159 Phylogenetic analysis was performed as described previously (17, 32, 33), with
160 minor modifications. Briefly, homologues and orthologues of the *pfbA* gene were
161 searched using tBLASTn (34). The sequences were aligned using Phylogears2 (35, 36)
162 and MAFFT v.7.221 with an L-INS-i strategy (37), and ambiguously aligned regions
163 were removed using Jalview (38, 39). The best-fitting codon evolutionary models for
164 phylogenetic analyses were determined using Kakusan4 (40). Bayesian Markov chain
165 Monte Carlo analyses were performed with MrBayes v.3.2.5 (41), and 4×10^6
166 generations were sampled after confirming that the standard deviation of split

frequencies was < 0.01 . To validate phylogenetic inferences, maximum likelihood phylogenetic analyses were performed with RAxML v.8.1.20 (42). Phylogenetic trees were generated using FigTree v.1.4.2 (43) based on the calculated data.

Human neutrophil and monocyte preparation

Human blood was obtained via venipuncture from healthy donors after obtaining informed consent. The protocol was approved by the institutional review boards of Osaka University Graduate School of Dentistry (H26-E43). Human neutrophils and monocytes were prepared using Polymorphprep (Alere Technologies AS, Oslo, Norway), according to the manufacturer's instructions. Human blood was carefully layered on the Polymorphprep solution in centrifugation tubes, which were then centrifuged at $450 \times g$ for 30 min in a swing-out rotor at 20°C. Monocyte and neutrophil fractions were transferred into tubes containing ACK buffer (0.15 M NH_4Cl , 0.01 M KHCO_3 , 0.1 mM EDTA), then centrifuged, washed in phosphate-buffered saline, and resuspended in RPMI 1640 medium.

183 **Neutrophil bactericidal assays**

184 The pneumococcal cells grown to the mid-log phase were resuspended in PBS.

185 TIGR4 strains ($3-11 \times 10^3$ CFUs/well) with or without rPfbA (0, 10, or 100 nM) were

186 combined with human neutrophils or neutrophil like-differentiated HL-60 cells (2×10^5

187 cells/well), and R6 strains ($1.4-2.0 \times 10^2$ CFUs/well) were combined with human

188 neutrophils (1×10^5 cells/well). The mixture was incubated at 37°C in 5% CO₂ for 1, 2,

189 and 3 h. Viable cell counts were determined by plating diluted samples onto TS blood

190 agar. The growth index was calculated as the number of CFUs at the specified time

191 point/number of CFUs in the initial inoculum. Bacterial phagocytosis was blocked by

192 addition of cytochalasin D (20 µM), and pneumococcal killing was blocked by protease

193 inhibitor cocktail set V (Merck, Darmstat, Germany; 500 µM AEBSF, 150 nM

194 Aprotinin, 1 µM E-64, and 1 µM leupeptin hemisulfate, EDTA-free) at 1 h before

195 incubation. To determine whether TLR2 and TLR4 signaling affect pneumococcal

196 survival, 100 µM TIRAP (TLR2 and TLR4) inhibitor peptide or control peptide (Novus

197 Biologicals) were added to neutrophils at 1 h before incubation.

198

Time-lapse microscopic analysis

For time-lapse observations, isolated neutrophils were resuspended in RPMI 1640 at 1×10^6 cells/mL. Next, 10 μ L of *S. pneumoniae* R6 wild type or $\Delta pfbA$ strains (1×10^6 CFUs) was added to 2 mL of the cells, and the mixture was incubated and observed at 37°C. Time-lapse images were captured using an Axio Observer Z1 microscope system (Carl Zeiss, Oberkochen, Germany).

Flow cytometric analysis of phagocytes

Recombinant PfbA (rPfbA) or BSA was coated onto 0.5- μ m-diameter fluorescent beads (FluoroSphere, Thermo Fisher Scientific), according to the manufacturer's instructions. rPfbA was purified as previously described (22). Isolated neutrophils or monocytes were then resuspended in RPMI 1640 at 1.0×10^7 cells/mL, after which 900 μ L of RPMI 1640 containing 1 μ L of rPfbA-, BSA-, or non-coated fluorescent beads was added to 100 μ L of cells, and then the mixtures were rotated at 37°C for 1 h. The cells were washed twice and fixed with 2% glutaraldehyde-RPMI 1640 at 37°C for 1 h, then washed again three times and analyzed with a CyFlow flow cytometer (Sysmex,

Hyogo, Japan) using FlowJo software ver. 8.3.2 (BD Biosciences, Franklin Lakes, NJ, USA).

TLR2/4 SEAPorter assay

HEK cells expressing TLR2 or TLR4 were stimulated with *S. pneumoniae* and/or rPfbA for 16 h, according to the manufacturer's instructions (Novus Biologicals). To avoid the effect of bacterial replication on this assay, *S. pneumoniae* were pasteurized by incubation at 56°C for 30 min. To perform the assay under the same condition, rPfbA was also incubated at 56°C for 30 min. Lipopolysaccharides from *Escherichia coli* O111:B4 (Sigma-Aldrich Japan Inc., Tokyo, Japan) for the TLR-4 cell line and Pam3CSK4 and Zymozan (Novus Biologicals) for the TLR-2 cell line were used as positive controls under the same conditions. Secreted alkaline phosphatase (SEAP) was analyzed using the SEAPorter Assay (Novus Biologicals) according to the manufacturer's instructions. Quantitative data (ng/mL) were obtained using a standard curve for the SEAP protein.

231 **RNA extraction and miRNA array**

232 We performed microRNA array analysis using neutrophil like-differentiated HL60
 233 cells incubated with *S. pneumoniae* strains and/or 100 nM rPfbA for 1 h. We compared
 234 rPfbA-treated and non-treated cells, wild type and $\Delta pfbA$ -infected cells, and $\Delta pfbA$ with
 235 and without rPfbA-infected cells. In each cell sample, six replicates were pooled and
 236 total RNA including microRNA was isolated from the pooled cells by miRNeasy Mini
 237 Kit (Qiagen, Hilden, Germany). Approximately 1000 ng RNA was used for microarray
 238 analysis using Affymetrix GeneChip miRNA 4.0 arrays (Affymetrix, Santa Clara, CA,
 239 USA) through Filgen Inc. (Nagoya, Japan). Briefly, the quality of total RNA was
 240 assessed using a Bioanalyzer 2100 (Agilent). Hybridization was performed using a
 241 FlashTag Biotin HSR RNA Labeling Kit, GeneChip Hybridization Oven 645, and
 242 GeneChip Fluidics Station 450. The arrays were scanned by Affymetrix GeneChip
 243 Scanner 3000 7G. The GeneChip miRNA 4.0 arrays contain 30,424 total mature
 244 miRNA probe sets including 2,578 mature human miRNAs, 2,025 pre-miRNA human
 245 probes, and 1,196 Human snoRNA and scaRNA probe sets.

246

247 **Mouse infection assays**

248 Mouse infection assays were performed as previously described (17, 33, 44, 45).

249 For the lung infection model, CD-1 mice (Slc:ICR, 8 weeks, female) were infected

250 intratracheally with $4.3\text{-}6.7 \times 10^6$ CFUs of *S. pneumoniae*. For intratracheal infection,

251 the vocal cords were visualized using an operating otoscope (Welch Allyn, NY, USA),

252 and 40 μL of bacteria was placed onto the trachea using a plastic gel loading pipette tip.

253 Mouse survival was monitored twice daily for 14 days. At 24 h after intratracheal

254 infection, bronchoalveolar lavage fluid (BALF) was collected following perfusion with

255 PBS.

256 For the sepsis model, CD-1 mice (Slc:ICR, 8 weeks, female) were infected

257 intravenously with $3.3\text{-}6.5 \times 10^5$ CFUs of *S. pneumoniae* via the tail vein. Mouse

258 survival was monitored twice daily for 14 days. At 24 and 48 h after infection, blood

259 aliquots were collected from mice following induction of general euthanasia. Brain,

260 lung, and liver samples were collected following perfusion with PBS. Brain and lung

261 whole tissues as well as the anterior segment of the liver were resected. Bacterial counts

262 in the blood as well as organ homogenates were determined by separately plating serial

dilutions, with organ counts corrected for differences in organ weight. Detection limits were 50 CFUs/organ and 50 CFUs/mL in blood.

The concentrations of TNF- α in BALF and plasma were determined using a Duoset[®] ELISA Kit (R&D Systems, Minneapolis, MN, USA). Mice plasma was obtained by centrifuging the heparinized blood. All mouse experiments were conducted in accordance with animal protocols approved by the Animal Care and Use Committees at Osaka University Graduate School of Dentistry (28-002-0).

Statistical analysis

Statistical analysis of *in vitro* and *in vivo* experiments was performed using a nonparametric analysis, Mann-Whitney *U* test, or Kruskal-Wallis test with Dunn's multiple comparisons test. Mouse survival curves were compared using a log-rank test. $p < 0.05$ was considered to indicate a significant difference. The tests were carried out with Graph Pad Prism version 6.0h (GraphPad Software, Inc., San Diego, CA, USA).

Results

The *pfbA* gene is specific to *S. pneumoniae* among mitis group *Streptococcus*

We searched *pfbA*-homologues by tBLASTn and performed phylogenetic analysis (Fig. 1 and Supplementary Fig. 1). The *pfbA* gene homologues were identified in *S. pneumoniae*, *Streptococcus pseudopneumoniae*, and *Streptococcus merionis*. Although 16S rRNA sequences cannot distinguish mitis group species, the 16S rRNA of *Streptococcus* sp. strain W10853 showed 99.387% identity to that of *S. pseudopneumoniae*. Interestingly, *S. pneumoniae*-related species such as *Streptococcus mitis* and *Streptococcus oralis* did not contain the homologues, whereas *S. merionis* had a gene of which the query cover and identity were over 50%. *S. merionis* strain NCTC13788 (also known as WUE3771, DSM 19192, and CCUG 54871), isolated from the oropharynges of Mongolian jirds (*Meriones unguiculatus*), contained 16S rRNA that belongs in a cluster distinct from the mitis group (46). This result indicates that the *pfbA* gene is specific to *S. pneumoniae* and *S. pseudopneumoniae* in the mitis group.

PfbA contributes to evasion of neutrophil killing

293 To investigate whether PfbA contributes to evasion of neutrophil killing, we
 294 determined pneumococcal survival rates after incubation with human neutrophils. After
 295 3 h incubation, the TIGR4 $\Delta pfbA$ strain showed a significantly decreased bacterial
 296 survival rate. In addition, to clarify whether the observed effects were attributed to PfbA,
 297 we also performed the assay with rPfbA. In the presence of 100 nM rPfbA, TIGR4
 298 $\Delta pfbA$ strain demonstrated a recovered survival rate nearly equal to that of the wild-type
 299 strain (Fig. 2A). In pneumococcal survival assays with neutrophil-like differentiated
 300 HL60 cells, TIGR4 strains showed similar results (Fig. 2B). We also performed the
 301 assay using the non-encapsulated strain R6 and human neutrophils. The R6 $\Delta pfbA$ strain
 302 showed significantly decreased survival rates as compared to the wild-type strain after
 303 incubation for 1, 2, and 3 h (Fig. 2C). As the R6 strain showed this phenotype at earlier
 304 time points than the TIGR4 strain, we performed pneumococcal survival assays using
 305 R6 strains with inhibitors (Fig. 2D). Neutrophil phagocytic killing of *S. pneumoniae*
 306 requires the serine proteases (47). Thus, we used a protein inhibitor cocktail as a
 307 positive control of a neutrophil killing inhibitor. While the R6 $\Delta pfbA$ strain showed
 308 significantly decreased survival rates at 1 h after incubation with human fresh

neutrophils in the absence of inhibitors, treatment with an actin polymerization inhibitor, cytochalasin D, reduced the differences among the wild-type and $\Delta pfbA$ strains as well as the protein inhibitor cocktail. These results indicate that PfbA contributes to pneumococcal evasion of neutrophil phagocytosis.

PfbA inhibits neutrophil phagocytosis directly

We confirmed the anti-phagocytic activity of PfbA using flow cytometry and PfbA-coated fluorescent beads (Fig. 3A). The fluorescence intensity of neutrophils and monocytes incubated with PfbA-coated beads was substantially lower as compared with cells incubated with non- or BSA-coated beads. These results indicated that neutrophils and monocytes phagocytosed the non- and BSA-coated fluorescent beads, whereas the PfbA-coated fluorescent beads escaped phagocytosis by neutrophils and monocytes.

We performed real-time observations for time-lapse analysis of the interaction between *S. pneumoniae* and neutrophils (Fig. 3B). *S. pneumoniae* strain R6 wild-type and $\Delta pfbA$ strains were separately incubated with fresh human neutrophils in RPMI 1640 medium. After coming into contact with neutrophils, the $\Delta pfbA$ strain was

phagocytosed within 1 min, whereas the wild-type strain was not phagocytosed after more than 5 min. Time-lapse analysis also showed the $\Delta pfbA$ strain engulfed by neutrophil phagosomes. These results suggest that PfbA can directly inhibit phagocytosis.

PfbA works as a TLR2 ligand and may inhibit phagocytosis through TLR2

Some lectins of pathogens work as ligand for TLR2 and TLR4 (48). We previously reported that PfbA can interact with glycolipid and glycoprotein fractions of red blood cells, several monosaccharides, D-sucrose, and D-raffinose (26, 27). Hence, to determine whether PfbA works as a TLR ligand, we performed a SEAP assay using HEK-293 cells stably transfected with either TLR2 or TLR4, NF- κ B, and SEAP (Fig. 4A). Pam3CSK4 and Zymozan were used as positive controls for the TLR2 ligand, while LPS was used for TLR4. The SEAP assay indicated that pasteurized *S. pneumoniae* TIGR4 wild-type cells activated NF- κ B via TLR2, whereas $\Delta pfbA$ cells did not stimulate cells expressing either TLR2 or TLR4. Pasteurized rPfbA also activated NF- κ B dose-dependently through TLR2, but not TLR4. In addition, in the presence of pasteurized rPfbA, $\Delta pfbA$

cells activated the cells expressing TLR2. Thus, PfbA is responsible for pneumococcal NF- κ B activation through TLR2.

Next, to determine whether TLR signaling suppresses survival of pneumococci incubated with neutrophils, we performed a neutrophil survival assay using a TIRAP inhibitor peptide (Fig. 4B). Data are presented as the ratio calculated by dividing CFUs in the presence of inhibitor peptide by CFUs in the presence of control peptide. TIRAP is an adaptor protein involved in MyD88-dependent TLR2 and TLR4 signaling pathways. Since the TIRAP inhibitor peptide blocks the interaction between TIRAP and TLRs, the peptide works as a TLR2 and TLR4 inhibitor. The inhibitor peptide treatment increased survival rates of the $\Delta pfbA$ strain, but did not affect wild-type survival rates. These results indicate that PfbA contributes to the evasion of neutrophil phagocytosis, and TIRAP inhibitor treatment did not change survival rates of pneumococci incubated with neutrophils. On the other hand, the *S. pneumoniae* $\Delta pfbA$ strain is more easily phagocytosed by neutrophils as compared to the wild-type strain, and this phenotype is abolished by TIRAP inhibitor.

356 Stimulation of the human monocytic cell line THP1 by a TLR ligand, LPS, induces
357 miR-146a/b expression in an NF- κ B-dependent fashion, and this induction inhibits
358 innate immune responses (49). In addition, pneumococcal infection of human
359 macrophages induces expression of several microRNAs, including miR-146a, in a
360 TLR-2-dependent manner, which prevents excessive inflammation (50). We performed
361 microRNA array analysis using neutrophil like-differentiated HL60 cells, *S.*
362 *pneumoniae* strains and rPfbA (Supplementary Fig. 2, Accession number: GSE128341).
363 We compared rPfbA-treated and non-treated cells, wild type and Δ *pfbA*-infected cells,
364 and Δ *pfbA* with and without rPfbA-infected cells. The analysis revealed only one
365 microRNA, hsa-miR-1281, that was commonly downregulated by 2-fold or greater in
366 the presence of PfbA as compared to in its absence (Supplementary Fig. 2, magenta
367 circle). On the other hand, there were no commonly upregulated miRNAs, including
368 miR-146a/b. In addition, the expression of eight microRNAs was commonly changed in
369 wild-type infection and Δ *pfbA* infection with rPfbA as compared to infection with
370 Δ *pfbA* only. Five micro RNAs (hsa-miR-4674, hsa-miR-3613-3p, hsa-miR-4668-5p,
371 hsa-miR-3197, and hsa-miR-6802-5p) were upregulated, while three (hsa-miR-3935,

hsa-miR-1281, and hsa-miR-3613-5p) were downregulated. However, the role of these miRNAs in infectious process remains unclear.

PfbA deficiency reduces pneumococcal burden in BALF but does not alter host survival rate in a mouse pneumonia model

To investigate the role of PfbA in pneumococcal pathogenesis, we infected mice with *S. pneumoniae* strains intratracheally and compared bacterial CFUs and TNF- α levels in BALF from mice 24 h after infection. There were no differences observed in survival time between mice infected with wild type and $\Delta pfbA$ strains (Fig. 5A). However, recovered CFUs of wild-type bacteria were significantly greater than those of $\Delta pfbA$ strains in mouse BALF. In addition, the level of TNF- α in BALF was almost the same in wild type and $\Delta pfbA$ infection (Fig. 5B).

PfbA deficiency increases pneumococcal pathogenicity in a mouse sepsis model

We also investigated the role of PfbA in mice following intravenous infection as a model of sepsis. In the infection model, the $\Delta pfbA$ strain showed significantly higher

388 levels of virulence as compared to the wild-type strain (Fig. 6A). Furthermore, we
389 compared the TNF- α levels in plasma and examined the bacterial burden in blood, brain,
390 lung, and liver samples obtained at 24 and 48 h after intravenous infection (Fig. 6B, 6C
391 and Supplementary Fig. 3). At 24 h after infection, TNF- α ELISA findings showed a
392 significantly greater level in the plasma of *pfbA* mutant strain-infected mice as
393 compared to the wild-type strain-infected mice. The numbers of CFUs of both the
394 wild-type and *pfbA* mutant strains in the blood and brain samples were comparable. On
395 the other hand, in the lung and liver samples, the *pfbA* mutant strain-infected mice
396 showed slightly but significantly reduced numbers of CFUs as compared with the
397 wild-type strain-infected mice. At 48 h after infection, there were no significant
398 differences in TNF- α level and bacterial burden in each organ between the wild-type-
399 and *pfbA* mutant strain-infected mice (Supplementary Fig. 3). Bacteria were not
400 detected in the blood of two of the wild-type strain-infected mice and five of the *pfbA*
401 mutant strain-infected mice. Meanwhile, three of the wild-type strain-infected mice
402 yielded more than 10^6 CFUs/mL, while seven of the wild-type strain-infected mice did.

403 The *pfbA* mutant strain infection caused a polarized bacterial burden in the host at 48 h
404 after infection as compared to wild type infection.

405 Discussion

406 In the present study, we found that *pfbA* is a pneumococcal-specific gene that
 407 contributes to evasion of neutrophil phagocytosis. We determined that PfbA can activate
 408 NF- κ B through TLR2. TIRAP inhibition increased the survival rate of Δ *pfbA* strain
 409 incubated with neutrophils, while this inhibition did not affect a wild-type strain
 410 survival. In a mouse model with lung infection, the bacterial burden of the Δ *pfbA* strain
 411 was significantly reduced as compared with that of wild-type strain, but the TNF- α level
 412 was comparable between the strains. Overall, there was no significant difference in the
 413 survival rates of mice infected with the wild-type *S. pneumoniae* strain- and those
 414 infected with the Δ *pfbA* strain. Furthermore, in a mouse model with blood infection, the
 415 Δ *pfbA* strain showed a significantly higher TNF- α level than the wild-type strain. These
 416 results suggest that PfbA may suppress the host innate immune response by acting as an
 417 anti-phagocytic factor interacting with TLR2.

418 Prior studies have shown that *S. pneumoniae* under selective pressure can adapt to
 419 the environment by importing genes from other related streptococci, such as those in the
 420 mitis group (51-54). Although *S. mitis* and *S. oralis* are oral commensal bacteria, these

species contain various pneumococcal virulence factor homologues. Some mitis group strains harbor several choline-binding proteins including autolysins, pneumolysin, sialidases, and others (11, 55, 56). In this study, we found that *pfbA* homologues were absent among mitis group strains without *S. pneumoniae* for which whole genome sequences were available, whereas the *pfbA* gene is highly conserved among pneumococcal strains. Interestingly, a streptococcal species with clear evolutionary separation from the mitis group, *S. merionis*, contained a *pfbA* orthologue. This result indicates that *pfbA* is a pneumococcal-specific gene and that ancestral *S. pneumoniae* likely obtained the gene by horizontal gene transfer from non-mitis group streptococcal species.

Although lipoproteins are major TLR2 ligands as well as peptidoglycans in *S. pneumoniae* (19), we found that rPfbA can activate NF- κ B solely in HEK293 cells expressing TLR2, but not those expressing TLR4. Since *E. coli* does not have the capacity to glycosylate proteins (57), rPfbA-mediated TLR2 activation would be independent of pneumococcal glycosylation. Plant and pathogen lectins can induce NF- κ B activation through binding to TLR2 *N*-glycans, while a classical ligand such as

Pam3CSK4 can activate NF- κ B glycan-independently (48). TLR2 has four *N*-glycans whose structures still remain unknown, and the *N*-glycans are critical for the lectins to induce TLR2-mediated activation (48). PfbA binds to various carbohydrates via the groove residues in the β -helix (26, 27). There is a possibility that PfbA induces TLR2 signaling by binding to TLR2 *N*-glycans.

Human macrophages challenged with *S. pneumoniae* induce a negative feedback loop, preventing excessive inflammation via miR-146a and potentially other miRNAs on the TLR2-MyD88 axis (50). On the other hand, pneumococcal endopeptidase O enhances macrophage phagocytosis in a TLR2- and miR-155-dependent manner (58). Furthermore, miR-9 is induced by TLR agonists and functions in feedback control of the NF- κ B-dependent responses in human monocytes and neutrophils (59). These studies indicate that host phagocytes are regulated by a complex combination of pattern recognition receptor signaling and miRNA induction. We predicted that PfbA suppresses phagocytosis via the induction of miRNAs in a TLR2 dependent fashion. However, an miRNA array showed that the levels of the involved miRNAs were not changed over 2-fold in the presence or absence of PfbA. One possible hypothesis is that

453 PfbA induces different miRNA responses from classical TLR ligands via
 454 glycan-dependent recognition. Although PfbA can downregulate miR-1281 in
 455 differentiated HL-60 cells, the role of miR-1281 in phagocytes remains unclear. Further
 456 comprehensive studies are required to investigate the role of miRNAs in host innate
 457 immunity.

458 Unexpectedly, our mouse pneumonia and sepsis models indicated that *pfbA*
 459 deficiency reduces pneumococcal survival in the host, but does not decrease or
 460 increases host mortality. We previously reported that PfbA works as an adhesin and
 461 invasin of host epithelial cells (22). The reduction of bacterial burden in host organs can
 462 be explained by the synergy of adhesive and anti-phagocytic abilities. On the other hand,
 463 the *S. pneumoniae* $\Delta pfbA$ strain showed equivalent or greater induction of inflammatory
 464 cytokines as compared with the wild-type strain. Generally, a deficiency of TLR ligands
 465 would suppress inflammatory responses. However, a deficiency of PfbA would cause
 466 more efficient bacterial uptake by phagocytes and promote inflammatory responses. In
 467 addition, there is a possibility that the negative feedback loop induced by PfbA is lost
 468 and causes excess inflammation. High mortality does not mean bacterial success, as

host death leads to the limitation of bacterial reproduction. PfbA may be beneficial for pneumococcal species by increasing the bacterial reproductive number through suppression of host cell phagocytosis and host mortality. PfbA showed high specificity for and conservation in *S. pneumoniae* species. The assumed negative feedback loop may not be as significant in non-pathogenic mitis group *Streptococcus*.

In single toxin-induced infectious diseases such as diphtheria and tetanus, highly safe and protective vaccines are established. On the other hand, in multiple factor-induced diseases such as those caused by *S. pneumoniae*, *S. pyogenes*, and so on, there are either no approved vaccines or existing vaccines still need optimization. Our study indicates that PfbA is a pneumococcal specific cell surface protein, which contributes to evasion from phagocytosis. Therefore, PfbA would not be suitable as a vaccine antigen, since the protein suppresses pneumococcal virulence in a mouse sepsis model. Further investigation of the intricate balance between host immunity and pathogenesis is required to establish the basis for drug and vaccine design.

484 **Acknowledgements**

485 This study was supported by the Japanese Society for the Promotion of Science
486 (JSPS), KAKENHI [grant numbers 26861546, 15H05012, 16H05847, 16K15787,
487 17H05103, 17K11666, and 18K19643], the SECOM Science and Technology
488 Foundation, Takeda Science Foundation, GSK Japan Research Grant, Asahi Glass
489 Foundation, Kurata Memorial Hitachi Science and Technology Foundation, Kobayashi
490 International Scholarship Foundation, and the Naito Foundation.

491

492 **Author contributions**

493 M.Y. and S.K. designed the study. M.Y. performed bioinformatics analyses. M.Y.,
494 Y.H., M.T., and M.O. performed the experiments. M.Y., T.S., M.N., Y.T., and S.K.
495 contributed to the setup of the experiments. M.Y. wrote the manuscript. Y.H., M.T.,
496 M.O., T.S., M.N., Y.T., and S.K. contributed to the writing of the manuscript.

497

498 **Conflict of interest**

499 The authors declare that they have no competing interests.

References

1. Kawamura Y, Hou XG, Sultana F, Miura H, Ezaki T. 1995. Determination of 16S rRNA sequences of *Streptococcus mitis* and *Streptococcus gordonii* and phylogenetic relationships among members of the genus *Streptococcus*. Int J Syst Evol Microbiol 45:406-8.
2. Richards VP, Palmer SR, Pavinski Bitar PD, Qin X, Weinstock GM, Highlander SK, Town CD, Burne RA, Stanhope MJ. 2014. Phylogenomics and the dynamic genome evolution of the genus *Streptococcus*. Genome Biol Evol 6:741-53.
3. Bogaert D, van Belkum A, Sluijter M, Luijendijk A, de Groot R, Rumke HC, Verbrugh HA, Hermans PW. 2004. Colonisation by *Streptococcus pneumoniae* and *Staphylococcus aureus* in healthy children. Lancet 363:1871-2.
4. Collaborators GL. 2017. Estimates of the global, regional, and national morbidity, mortality, and aetiologies of lower respiratory tract infections in 195 countries: a systematic analysis for the Global Burden of Disease Study 2015. Lancet Infect Dis 17:1133-1161.
5. McIntyre PB, O'Brien KL, Greenwood B, van de Beek D. 2012. Effect of vaccines on bacterial meningitis worldwide. Lancet 380:1703-11.
6. WHO. 2017. WHO priority pathogens list for R&D of new antibiotics. <http://www.who.int/mediacentre/news/releases/2017/bacteria-antibiotics-needed/en/>. Accessed
7. Kim L, McGee L, Tomczyk S, Beall B. 2016. Biological and Epidemiological Features of Antibiotic-Resistant *Streptococcus pneumoniae* in Pre- and Post-Conjugate Vaccine Eras: a United States Perspective. Clin Microbiol Rev 29:525-52.
8. Golubchik T, Brueggemann AB, Street T, Gertz RE, Jr., Spencer CC, Ho T, Giannoulatou E, Link-Gelles R, Harding RM, Beall B, Peto TE, Moore MR, Donnelly P, Crook DW, Bowden R. 2012. Pneumococcal genome sequencing tracks a vaccine escape variant formed through a multi-fragment recombination event. Nat Genet 44:352-5.
9. Flasche S, Van Hoek AJ, Sheasby E, Waight P, Andrews N, Sheppard C, George R, Miller E. 2011. Effect of pneumococcal conjugate vaccination on serotype-specific carriage and invasive disease in England: a cross-sectional

- study. PLoS Med 8:e1001017.
10. Lofling J, Vimberg V, Battig P, Henriques-Normark B. 2011. Cellular interactions by LPxTG-anchored pneumococcal adhesins and their streptococcal homologues. Cell Microbiol 13:186-97.
11. Hakenbeck R, Madhour A, Denapaite D, Bruckner R. 2009. Versatility of choline metabolism and choline-binding proteins in *Streptococcus pneumoniae* and commensal streptococci. FEMS Microbiol Rev 33:572-86.
12. Mitchell AM, Mitchell TJ. 2010. *Streptococcus pneumoniae*: virulence factors and variation. Clin Microbiol Infect 16:411-8.
13. Weiser JN, Ferreira DM, Paton JC. 2018. *Streptococcus pneumoniae*: transmission, colonization and invasion. Nat Rev Microbiol 16:355-367.
14. Ren B, McCrory MA, Pass C, Bullard DC, Ballantyne CM, Xu Y, Briles DE, Szalai AJ. 2004. The virulence function of *Streptococcus pneumoniae* surface protein A involves inhibition of complement activation and impairment of complement receptor-mediated protection. J Immunol 173:7506-12.
15. Dave S, Carmicle S, Hammerschmidt S, Pangburn MK, McDaniel LS. 2004. Dual roles of PspC, a surface protein of *Streptococcus pneumoniae*, in binding human secretory IgA and factor H. J Immunol 173:471-7.
16. Gutierrez-Fernandez J, Saleh M, Alcorlo M, Gomez-Mejia A, Pantoja-Uceda D, Trevino MA, Voss F, Abdullah MR, Galan-Bartual S, Seinen J, Sanchez-Murcia PA, Gago F, Bruix M, Hammerschmidt S, Hermoso JA. 2016. Modular Architecture and Unique Teichoic Acid Recognition Features of Choline-Binding Protein L (CbpL) Contributing to Pneumococcal Pathogenesis. Sci Rep 6:38094.
17. Yamaguchi M, Goto K, Hirose Y, Yamaguchi Y, Sumitomo T, Nakata M, Nakano K, Kawabata S. 2019. Identification of evolutionarily conserved virulence factor by selective pressure analysis of *Streptococcus pneumoniae*. Commun Biol 2:96.
18. Koppe U, Suttrop N, Opitz B. 2012. Recognition of *Streptococcus pneumoniae* by the innate immune system. Cell Microbiol 14:460-6.
19. Tomlinson G, Chimalapati S, Pollard T, Lapp T, Cohen J, Camberlein E, Stafford S, Periselneris J, Aldridge C, Vollmer W, Picard C, Casanova JL, Noursadeghi M, Brown J. 2014. TLR-mediated inflammatory responses to *Streptococcus pneumoniae* are highly dependent on surface expression of

- 565 bacterial lipoproteins. J Immunol 193:3736-45.
- 566 20. Sabroe I, Dower SK, Whyte MK. 2005. The role of Toll-like receptors in the
567 regulation of neutrophil migration, activation, and apoptosis. Clin Infect Dis 41
568 Suppl 7:S421-6.
- 569 21. Richard AL, Siegel SJ, Erikson J, Weiser JN. 2014. TLR2 signaling decreases
570 transmission of *Streptococcus pneumoniae* by limiting bacterial shedding in an
571 infant mouse Influenza A co-infection model. PLoS Pathog 10:e1004339.
- 572 22. Yamaguchi M, Terao Y, Mori Y, Hamada S, Kawabata S. 2008. PfbA, a novel
573 plasmin- and fibronectin-binding protein of *Streptococcus pneumoniae*,
574 contributes to fibronectin-dependent adhesion and antiphagocytosis. J Biol
575 Chem 283:36272-9.
- 576 23. Yamaguchi M. 2018. Synergistic findings from microbiological and evolutionary
577 analyses of virulence factors among pathogenic streptococcal species. Journal of
578 Oral Biosciences 60:36-40.
- 579 24. Suits MD, Boraston AB. 2013. Structure of the *Streptococcus pneumoniae*
580 surface protein and adhesin PfbA. PLoS One 8:e67190.
- 581 25. Beulin DS, Yamaguchi M, Kawabata S, Ponnuraj K. 2014. Crystal structure of
582 PfbA, a surface adhesin of *Streptococcus pneumoniae*, provides hints into its
583 interaction with fibronectin. Int J Biol Macromol 64:168-73.
- 584 26. Beulin DSJ, Radhakrishnan D, Suresh SC, Sadasivan C, Yamaguchi M,
585 Kawabata S, Ponnuraj K. 2017. *Streptococcus pneumoniae* surface protein PfbA
586 is a versatile multidomain and multiligand-binding adhesin employing different
587 binding mechanisms. FEBS J 284:3404-3421.
- 588 27. Radhakrishnan D, Yamaguchi M, Kawabata S, Ponnuraj K. 2018. *Streptococcus*
589 *pneumoniae* surface adhesin PfbA and its interaction with erythrocytes and
590 hemoglobin. Int J Biol Macromol 120:135-143.
- 591 28. Mori Y, Yamaguchi M, Terao Y, Hamada S, Ooshima T, Kawabata S. 2012.
592 α -Enolase of *Streptococcus pneumoniae* induces formation of neutrophil
593 extracellular traps. J Biol Chem 287:10472-81.
- 594 29. Bricker AL, Camilli A. 1999. Transformation of a type 4 encapsulated strain of
595 *Streptococcus pneumoniae*. FEMS Microbiol Lett 172:131-5.
- 596 30. Collins SJ, Ruscetti FW, Gallagher RE, Gallo RC. 1979. Normal functional
597 characteristics of cultured human promyelocytic leukemia cells (HL-60) after

- p>induction of differentiation by dimethylsulfoxide. J Exp Med 149:969-74.
p>31. Wen X, Jin T, Xu X. 2016. Imaging G Protein-coupled Receptor-mediated Chemotaxis and its Signaling Events in Neutrophil-like HL60 Cells. J Vis Exp doi:10.3791/54511.
p>32. Yamaguchi M, Hirose Y, Nakata M, Uchiyama S, Yamaguchi Y, Goto K, Sumitomo T, Lewis AL, Kawabata S, Nizet V. 2016. Evolutionary inactivation of a sialidase in group B
- Streptococcus*
- . Sci Rep 6:28852.
p>33. Yamaguchi M, Nakata M, Sumioka R, Hirose Y, Wada S, Akeda Y, Sumitomo T, Kawabata S. 2017. Zinc metalloproteinase ZmpC suppresses experimental pneumococcal meningitis by inhibiting bacterial invasion of central nervous systems. Virulence 8:1516-1524.
p>34. Gertz EM, Yu YK, Agarwala R, Schaffer AA, Altschul SF. 2006. Composition-based statistics and translated nucleotide searches: improving the TBLASTN module of BLAST. BMC Biol 4:41.
p>35. Tanabe AS. 2008. Phylogears2 ver. 2.0.
- <http://www.fifthdimension.jp/>
- . Accessed
p>36. Venditti C, Meade A, Pagel M. 2006. Detecting the node-density artifact in phylogeny reconstruction. Syst Biol 55:637-43.
p>37. Katoh K, Standley DM. 2013. MAFFT multiple sequence alignment software version 7: improvements in performance and usability. Mol Biol Evol 30:772-80.
p>38. Waterhouse AM, Procter JB, Martin DM, Clamp M, Barton GJ. 2009. Jalview Version 2--a multiple sequence alignment editor and analysis workbench. Bioinformatics 25:1189-91.
p>39. Talavera G, Castresana J. 2007. Improvement of phylogenies after removing divergent and ambiguously aligned blocks from protein sequence alignments. Syst Biol 56:564-77.
p>40. Tanabe AS. 2011. Kakusan4 and Aminosan: two programs for comparing nonpartitioned, proportional and separate models for combined molecular phylogenetic analyses of multilocus sequence data. Mol Ecol Resour 11:914-21.
p>41. Ronquist F, Teslenko M, van der Mark P, Ayres DL, Darling A, Hohna S, Larget B, Liu L, Suchard MA, Huelsenbeck JP. 2012. MrBayes 3.2: efficient Bayesian phylogenetic inference and model choice across a large model space. Syst Biol

631 61:539-42.

632 42. Stamatakis A. 2014. RAxML version 8: a tool for phylogenetic analysis and
633 post-analysis of large phylogenies. *Bioinformatics* 30:1312-3.

634 43. Rambaut A. 2014. FigTree ver.1.4.2.
635 <http://tree.bio.ed.ac.uk/software/figtree/>. Accessed

636 44. Okerblom JJ, Schwarz F, Olson J, Fletes W, Ali SR, Martin PT, Glass CK, Nizet
637 V, Varki A. 2017. Loss of CMAH during Human Evolution Primed the
638 Monocyte-Macrophage Lineage toward a More Inflammatory and Phagocytic
639 State. *J Immunol* 198:2366-2373.

640 45. Hirose Y, Yamaguchi M, Goto K, Sumitomo T, Nakata M, Kawabata S. 2018.
641 Competence-induced protein Ccs4 facilitates pneumococcal invasion into brain
642 tissue and virulence in meningitis. *Virulence* 9:1576-1587.

643 46. Tappe D, Pukall R, Schumann P, Gronow S, Spiliotis M, Claus H, Brehm K,
644 Vogel U. 2009. *Streptococcus merionis* sp. nov., isolated from *Mongolian jirds*
645 (*Meriones unguiculatus*). *Int J Syst Evol Microbiol* 59:766-70.

646 47. Standish AJ, Weiser JN. 2009. Human neutrophils kill *Streptococcus*
647 *pneumoniae* via serine proteases. *J Immunol* 183:2602-9.

648 48. Ricci-Azevedo R, Roque-Barreira MC, Gay NJ. 2017. Targeting and
649 Recognition of Toll-Like Receptors by Plant and Pathogen Lectins. *Front*
650 *Immunol* 8:1820.

651 49. Taganov KD, Boldin MP, Chang KJ, Baltimore D. 2006. NF- κ B-dependent
652 induction of microRNA miR-146, an inhibitor targeted to signaling proteins of
653 innate immune responses. *Proc Natl Acad Sci U S A* 103:12481-6.

654 50. Griss K, Bertrams W, Sittka-Stark A, Seidel K, Stielow C, Hippenstiel S, Suttorp
655 N, Eberhardt M, Wilhelm J, Vera J, Schmeck B. 2016. MicroRNAs Constitute a
656 Negative Feedback Loop in *Streptococcus pneumoniae*-Induced Macrophage
657 Activation. *J Infect Dis* 214:288-99.

658 51. Bek-Thomsen M, Poulsen K, Kilian M. 2012. Occurrence and evolution of the
659 paralogous zinc metalloproteases IgA1 protease, ZmpB, ZmpC, and ZmpD in
660 *Streptococcus pneumoniae* and related commensal species. *MBio* 3: e00303-12.

661 52. Kilian M, Riley DR, Jensen A, Bruggemann H, Tettelin H. 2014. Parallel
662 evolution of *Streptococcus pneumoniae* and *Streptococcus mitis* to pathogenic
663 and mutualistic lifestyles. *MBio* 5:e01490-14.

53. Jensen A, Valdorsson O, Frimodt-Moller N, Hollingshead S, Kilian M. 2015. Commensal streptococci serve as a reservoir for β -lactam resistance genes in *Streptococcus pneumoniae*. *Antimicrob Agents Chemother* 59:3529-40.
54. Skov Sorensen UB, Yao K, Yang Y, Tettelin H, Kilian M. 2016. Capsular Polysaccharide Expression in Commensal *Streptococcus* Species: Genetic and Antigenic Similarities to *Streptococcus pneumoniae*. *MBio* 7:e01844-16.
55. Kilian M, Poulsen K, Blomqvist T, Havarstein LS, Bek-Thomsen M, Tettelin H, Sorensen UB. 2008. Evolution of *Streptococcus pneumoniae* and its close commensal relatives. *PLoS One* 3:e2683.
56. Johnston C, Hinds J, Smith A, van der Linden M, Van Eldere J, Mitchell TJ. 2010. Detection of large numbers of pneumococcal virulence genes in streptococci of the mitis group. *J Clin Microbiol* 48:2762-9.
57. Clausen H, Wandall HH, Steentoft C, Stanley P, Schnaar RL. 2015. Glycosylation Engineering, p 713-728. In Varki A, Cummings RD, Esko JD, Stanley P, Hart GW, Aebi M, Darvill AG, Kinoshita T, Packer NH, Prestegard JH, Schnaar RL, Seeberger PH (ed), *Essentials of Glycobiology*, 3rd edition doi:10.1101/glycobiology.3e.056. Cold Spring Harbor Laboratory Press, New York.
58. Yao H, Zhang H, Lan K, Wang H, Su Y, Li D, Song Z, Cui F, Yin Y, Zhang X. 2017. Purified *Streptococcus pneumoniae* Endopeptidase O (PepO) Enhances Particle Uptake by Macrophages in a Toll-Like Receptor 2- and miR-155-Dependent Manner. *Infect Immun* 85.
59. Bazzoni F, Rossato M, Fabbri M, Gaudiosi D, Mirolo M, Mori L, Tamassia N, Mantovani A, Cassatella MA, Locati M. 2009. Induction and regulatory function of miR-9 in human monocytes and neutrophils exposed to proinflammatory signals. *Proc Natl Acad Sci U S A* 106:5282-7.

Figure Legends

Figure 1. Bayesian phylogenetic analysis of the *pfbA* gene.

The codon-based Bayesian phylogenetic relationship was calculated using the MrBayes program. Strains with identical sequences are listed on the same branch. The percentage of posterior probabilities is shown near the nodes. The scale bar indicates nucleotide substitutions per site.

Figure 2. PfbA contributes to pneumococcal survival after incubation with

neutrophils. A. Growth of TIGR4 strains incubated with human fresh neutrophils. **B.**

Growth of TIGR4 strains incubated with neutrophil-like differentiated HL-60 cells.

Bacterial cells were incubated with human neutrophils or differentiated HL-60 cells in

the presence or absence of rPfbA for 1, 2, and 3 h at 37°C in a 5% CO₂ atmosphere.

Next, the mixture was serially diluted and plated on TS blood agar. Following

incubation, the number of CFUs was determined. Growth index was calculated by

dividing CFUs after incubation by CFUs of the original inoculum. **C.** Growth of R6

strains incubated with human fresh neutrophils. *S. pneumoniae* strains were added to

human neutrophils without serum and gently mixed for 1, 2, or 3 h at 37°C. Next, the mixtures were serially diluted and plated on TS blood agar. After incubation, the number of CFUs was determined. **D.** Growth of R6 strains incubated with human fresh neutrophils in the presence of inhibitors. *S. pneumoniae* strains were added to human neutrophils with or without cytochalasin D, or protease inhibitor cocktail in the absence of serum, then gently mixed for 1 h at 37°C. The percent bacterial survival was calculated based on viable counts relative to the wild-type strain. These data are presented as the mean values of six samples, with S.E. values represented by vertical lines. Differences between several groups were analyzed using a Kruskal-Wallis test followed by Dunn's multiple comparisons test (A, B). The Mann-Whitney's U test was used to compare differences between two independent groups (C, D). Three experiments were performed, with data from a representative experiment is shown.

Figure 3. PfbA suppresses host cell phagocytosis. A. Uptake of fluorescent PfbA-coated beads by neutrophils and monocytes. Human neutrophils and monocytes were separately incubated with PfbA-, BSA-, or non-coated fluorescent beads for 1 h at

37°C. Phagocytic activities were analyzed using flow cytometry. Data are presented as histograms. The value shown for the percent of maximum was determined by dividing the number of cells in each bin by the number of cells in the bin that contained the largest number of cells. The bin is shown as a numerical range for the parameter on the X-axis. **B.** Time-lapse analysis of the interaction between *S. pneumoniae* and neutrophils. *S. pneumoniae* wild-type and $\Delta pfbA$ strains were incubated with neutrophils. The elapsed times from contact with neutrophils are shown in the upper part of the figures. Arrows indicate when *S. pneumoniae* cells contacted neutrophils. Arrowheads indicate *S. pneumoniae* engulfed by a neutrophil phagosome.

Figure 4. PfbA activates NF- κ B via TLR2, and TLR2/4 inhibitor enhances $\Delta pfbA$ strain survival. **A.** Secreted alkaline phosphatase (SEAP) porter assay using TLR2/NF- κ B/ SEAPorter or TLR4/MD-2/CD14/NF- κ B SEAPorter HEK293 cell lines. The cells were plated in 24-well plates at 5×10^5 cells/well. After 24 h, cells were stimulated with various amount of rPfbA, pasteurized *S. pneumoniae* ($\sim 5 \times 10^6$ CFU), 1 μ g/mL Pam3CSK4, 10 μ g/mL Zymozan, or 25 ng/mL LPS for 24 h. SEAP was

analyzed using the SEAPorter Assay Kit. Data are presented as the mean of six wells. SE values are represented by vertical lines. Differences in pneumococcal infection group and rPfbA addition group were analyzed using a Kruskal-Wallis test followed by Dunn's multiple comparisons test, respectively. **B.** TLR2/4 inhibitor peptide enhances survival of the TIGR4 $\Delta pfbA$ strain incubated with human neutrophils. *S. pneumoniae* TIGR4 wild type strain or $\Delta pfbA$ strain bacteria were incubated with human neutrophils in the presence of TLR2/4 inhibitor peptide or control peptide. After 1, 2, and 3 h, the mixture was serially diluted and plated on TS blood agar. Following incubation, the number of CFUs was determined. The CFU ratio was calculated by dividing CFUs in the presence of inhibitor peptide by CFUs in the presence of control peptide. Data are presented as the mean of six wells. S.E. values are represented by vertical lines. Differences between groups were analyzed using Mann-Whitney's U test.

Figure 5. In a mouse pneumonia model, deficiency of *pfbA* decreases pneumococcal burden in the lung but does not affect host mortality. A. CD-1 mice were infected

756 intratracheally with the *S. pneumoniae* TIGR4 wild-type or $\Delta pfbA$ strain ($3-18 \times 10^6$
 757 CFUs). Mice survival was recorded for 14 days. The differences between groups were
 758 analyzed using a log-rank test. **B.** Bacterial CFUs and TNF- α in BALF collected from
 759 CD-1 mice after intratracheal infection with *S. pneumoniae*. CD-1 mice were infected
 760 intratracheally with the *S. pneumoniae* TIGR4 wild type or $\Delta pfbA$ strain ($4-7 \times 10^6$
 761 CFUs). BALF was collected at 24 h after pneumococcal infection, and bacterial CFUs
 762 and TNF- α levels in the BALF were determined. S.E. values are represented by vertical
 763 lines. Statistical differences between groups were analyzed using Mann-Whitney's U
 764 test. The data obtained from three independent experiments were pooled.

765

766 **Figure 6. In a mouse sepsis model, the deficiency of *pfbA* increases the virulence**
 767 **and TNF- α level in blood but decreases the bacterial burden in the lung and liver.**

768 CD-1 mice were infected intravenously with the *S. pneumoniae* TIGR4 wild type or
 769 $\Delta pfbA$ strain ($3-6 \times 10^6$ CFUs). **A.** Mouse survival was monitored for 14 days.
 770 Statistical differences between groups were analyzed using a log-rank test. **B.** CD-1
 771 mice were infected intravenously with the *S. pneumoniae* TIGR4 wild type or $\Delta pfbA$

772 strain ($6-9 \times 10^6$ CFUs). Plasma samples were collected from these mice at 24 h after
 773 infection. Values are presented as the mean of 16 or 18 samples. Vertical lines represent
 774 the mean \pm S.E. Statistical differences between groups were analyzed using
 775 Mann-Whitney's U test. **C.** The bacterial burden in the blood, brain, lung, and liver
 776 were assessed after 24 h of infection. S.E. values are represented by vertical lines. All
 777 mice were perfused with PBS after blood collection, organ samples were collected.
 778 Statistical differences between groups were analyzed using Mann-Whitney's U test. The
 779 mouse survival data were obtained from three independent experiments, and the TNF- α
 780 level and bacterial burden values obtained from two independent experiments were
 781 pooled.
 782

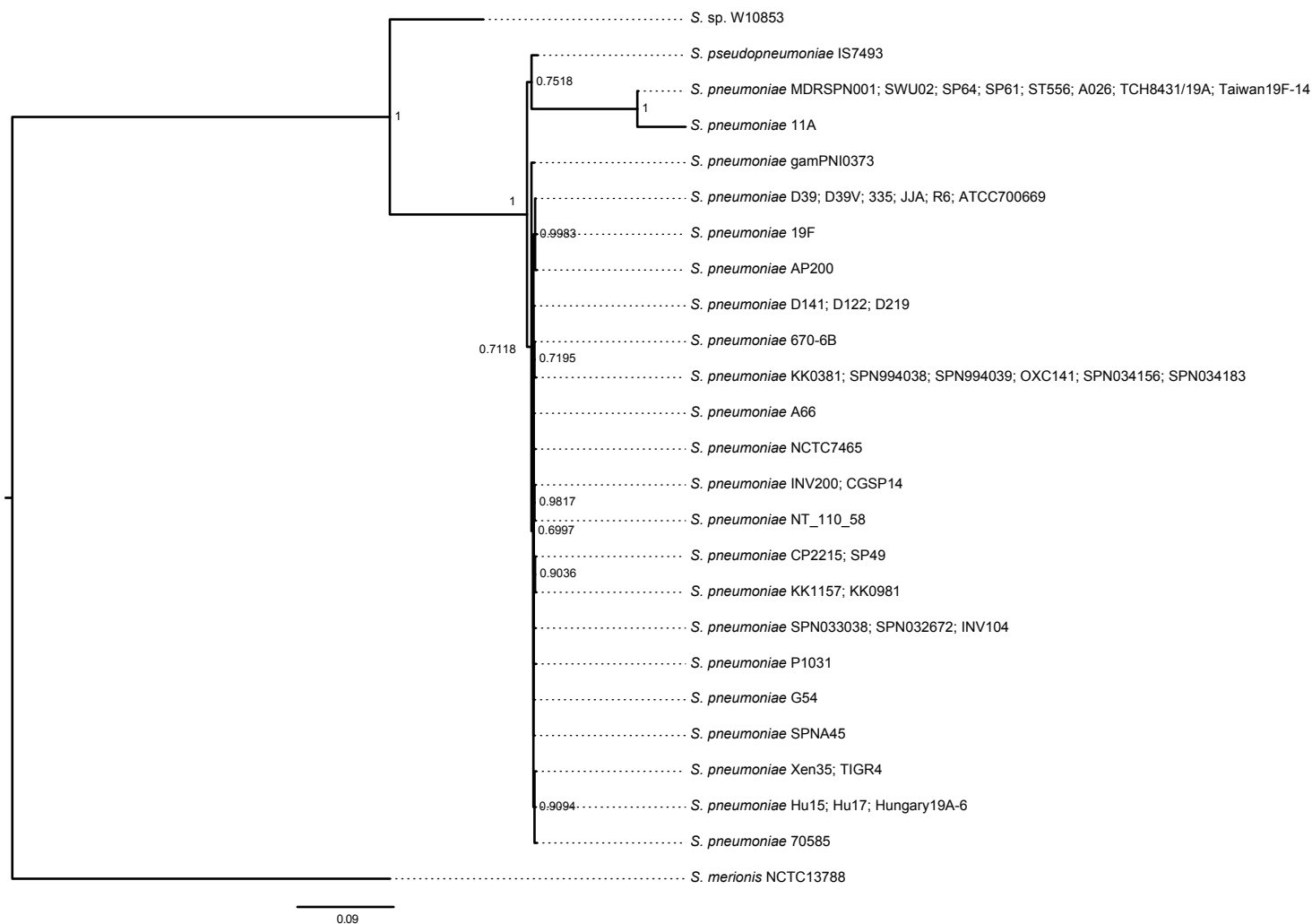


Figure 1. Yamaguchi *et al.*

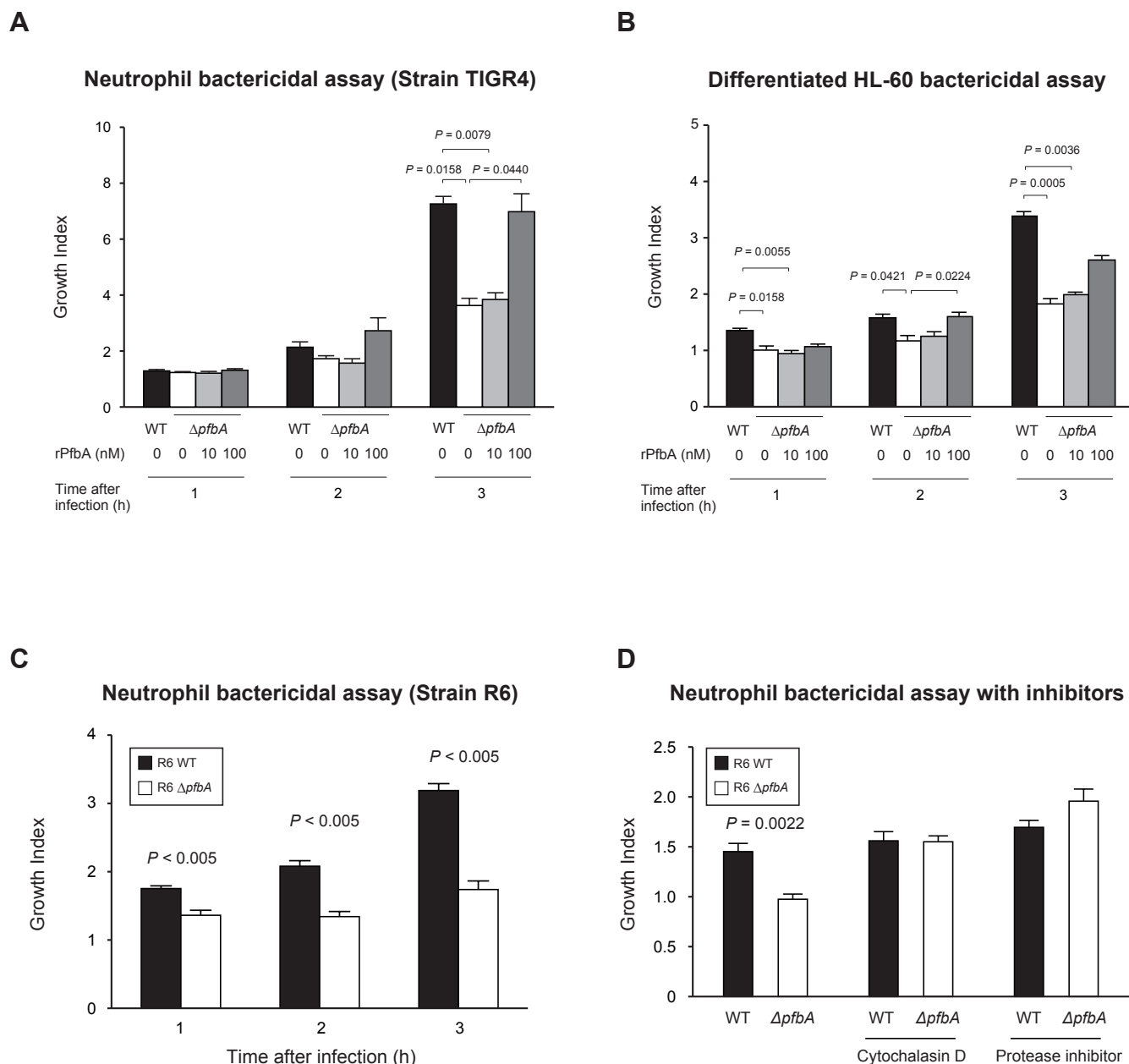
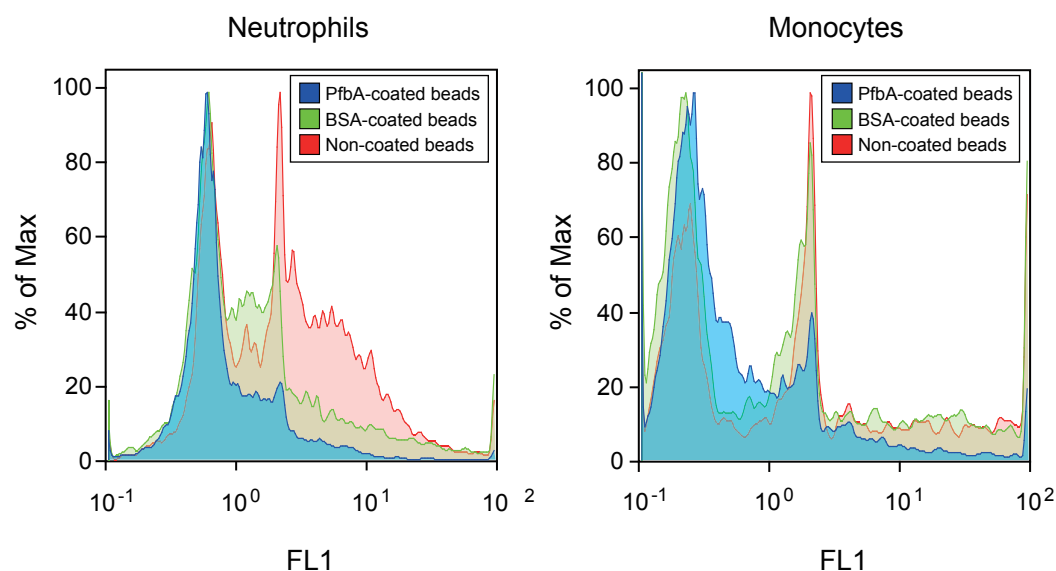


Figure 2. Yamaguchi *et al.*

A



B

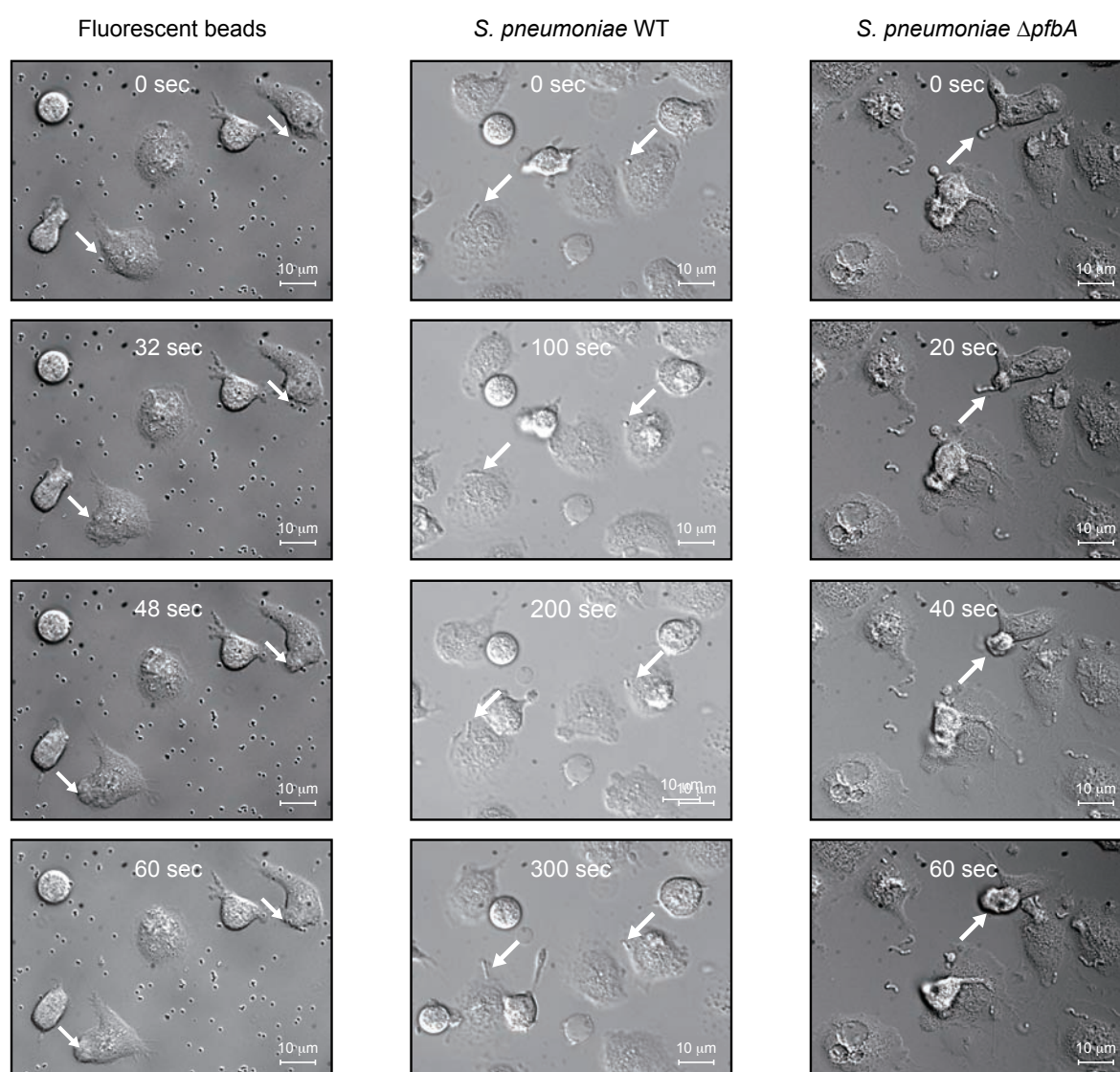
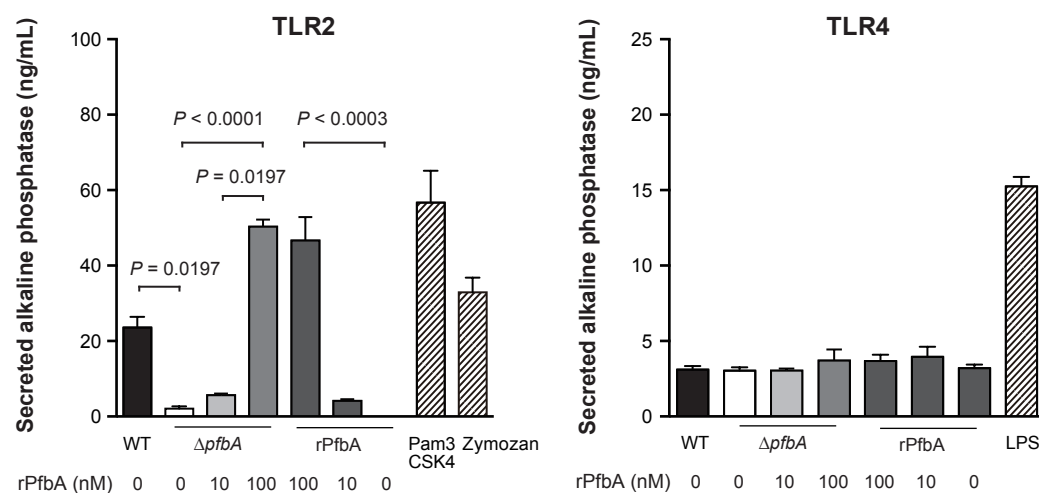


Figure 3. Yamaguchi *et al.*

A



B

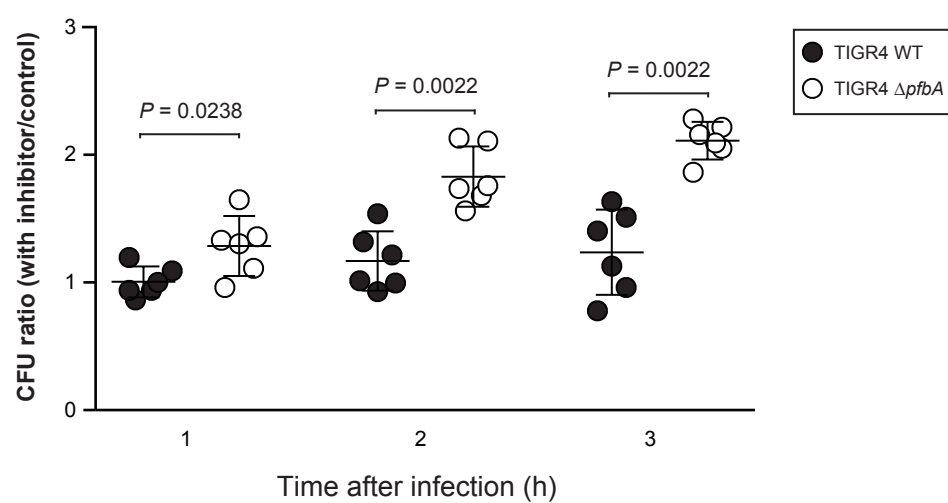
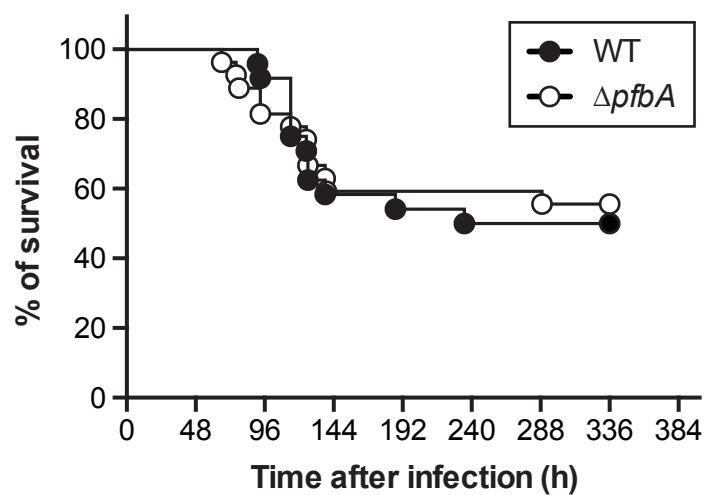


Figure 4. Yamaguchi *et al.*

A



B

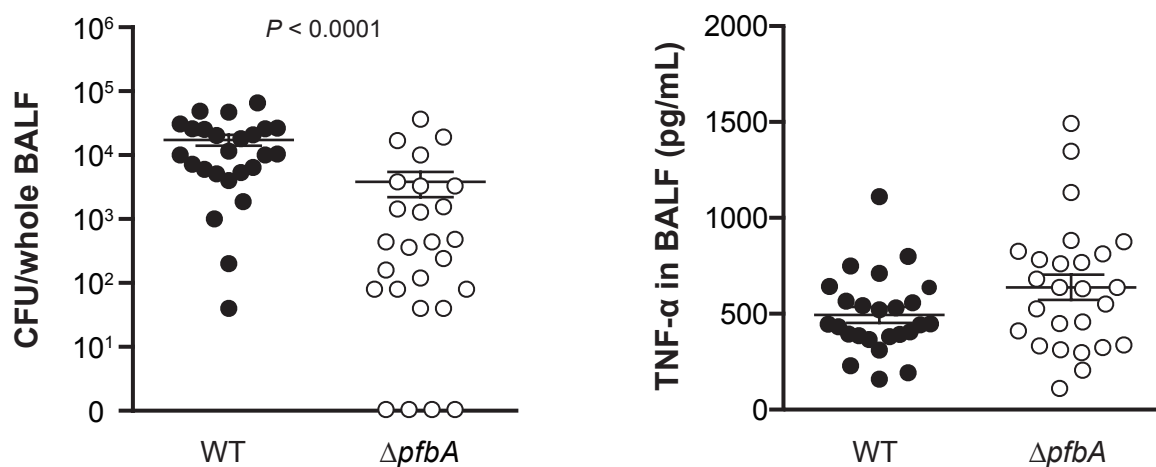


Figure 5. Yamaguchi *et al.*

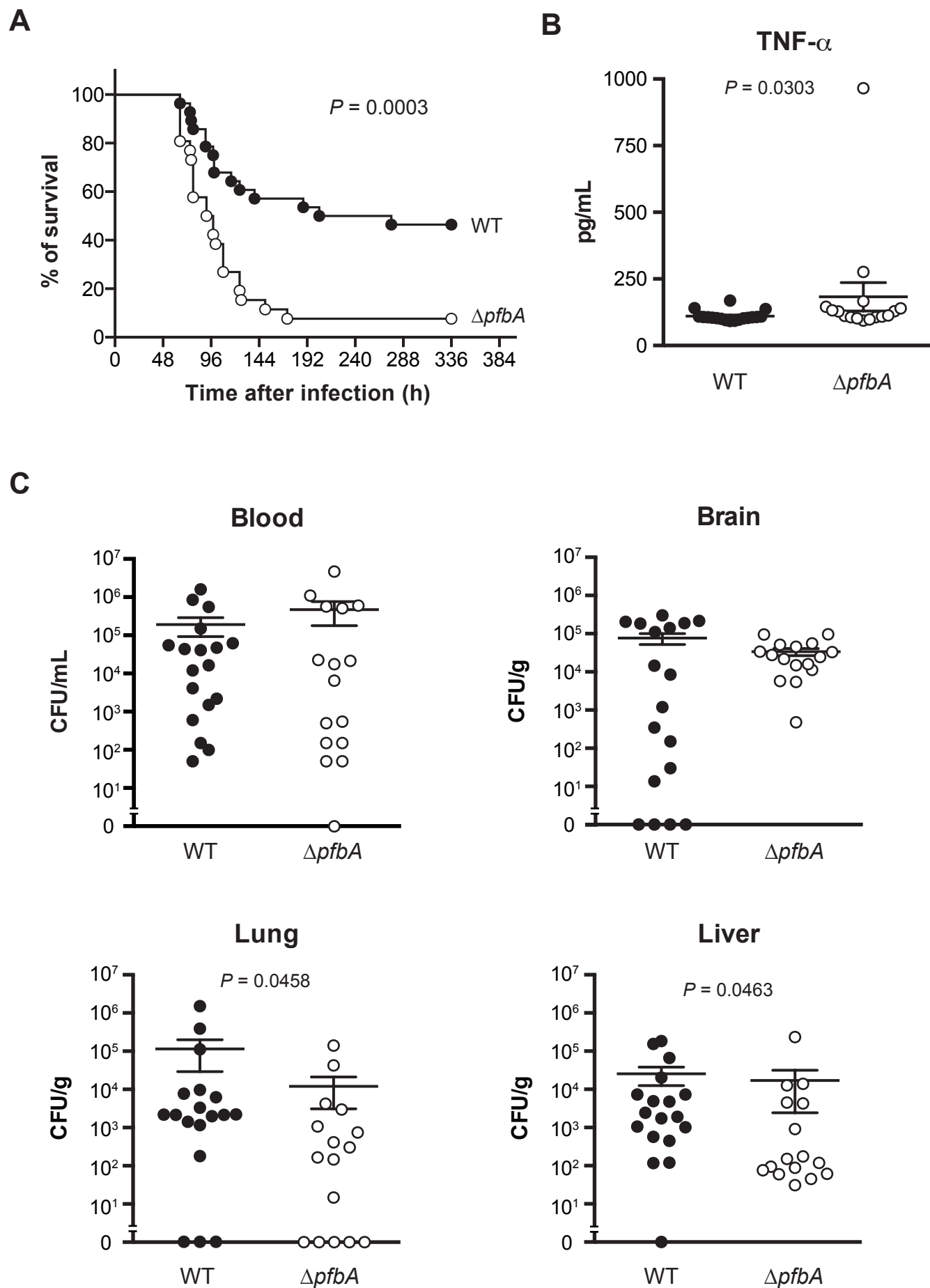


Figure 6. Yamaguchi *et al.*